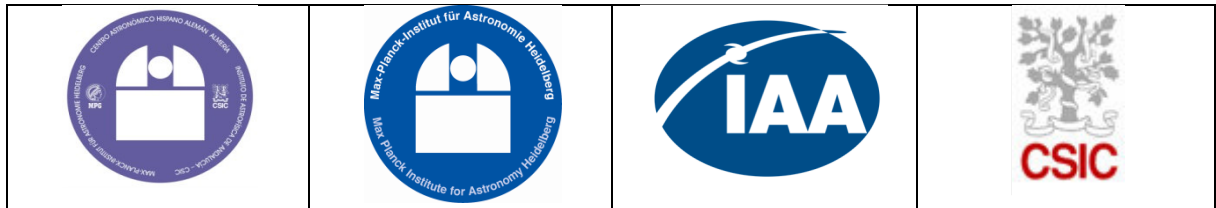


	PANIC4K detector characterization	Doc.Ref: PANIC4K-DET-TR-01 Issue: 1.0 Date: 30.05.2025 Page 1 / 33
---	--	---



PANIC4K

PANIC4K Detector characterization

Prepared by	Vianak Naranjo	Max-Planck-Institut für Astronomie
Checked by		

Code: PANIC4K-DET-TR-01
Issue/Ver.: 1.0
Date: 30.05.2025
No. of pages: 33

	PANIC4K detector characterization	Doc.Ref: PANIC4K-DET-TR-01 Issue: 1.0 Date: 30.05.2025 Page 2 / 33
---	--	---

Document Change Log

Version	Date	Chapters affected	Comments
Issue 1.0	30.05.2025	All	Final version

List of acronyms and abbreviations


ADU	Analog-Digital Unit
AVG	Average
CAHA	Centro Astronómico Hispano en Andalucía
CDS	Correlated Double Sampling
cntsr	continuous sampling read
DIT	Detector integration time
Dsub	Detector Substrate Voltage
FPA	Focal Plane Array
GEIRS	GEneric InfraRed Software
H4RG	Hawaii 4 RG
IAA	Instituto de Astrofísica de Andalucía
itime	Integration time
MPIA	Max-Planck-Institut für Astronomie
PANIC	PA noramic N ear Infrared camera for C alar Alto
PTC	Photon Transfer Curve
QE	Quantum Efficiency
ROE	Read-out Electronics
RON	Read-out Noise
Rlr	Reset level read
RwoC	Read without Conversion
SG	Science Grade
Vbias gate	Bias gate supply voltage
Vbias power	Bias power supply voltage
Vext.bias	External bias supply voltage
Vreset	Reset voltage

	PANIC4K detector characterization	Doc.Ref: PANIC4K-DET-TR-01 Issue: 1.0 Date: 30.05.2025 Page 3 / 33
---	--	---

List of supporting documents

The following documents provide additional information about topics addressed in this document. They are referenced as RDx in the text:

RD Nr.	Identifier	Title	Issue	Date
RD1	PANIC4K-DET-TN-01	PANIC4K History of Events	1.0	09.10.2024
RD2	PANIC4K-DET-TN-02	PANIC4K detector non-linearity correction data	Draft	08.04.2025
RD3	H4RG-19908-IR25-TIS	Post Repair and Diagnostics Test Report (Teledyne)		09.07.2021
RD4	Vol. 8453 of Proc. SPIE, Int. Soc. Optical Engineering, 2012, p. 2E.	Standard modes of MPIA's current H2/H2RG-readout systems		2012
RD5	PANIC-GEN-SP-01	PANIC Preliminary Design Report	0/1	22.10.2007
RD6	PANIC4K-DET-TN-03	Electronic CDS offset	1.0	09.04.2025
RD7	PANIC-SW-DCS-01	Generic Infrared Software – Installation and User's Manual	12.146	26.05.2025

	PANIC4K detector characterization	Doc.Ref: PANIC4K-DET-TR-01 Issue: 1.0 Date: 30.05.2025 Page 4 / 33
---	--	---

Contents

1	Introduction and scope	5
1.1	General	5
1.2	Discussed items	5
2	Setup and data	5
2.1	Instrument setup	5
2.2	Detector setup.....	5
2.3	GEIRS Versions and minimum integration times	6
2.4	Data	6
3	Summary	6
4	Reset level drift.....	7
5	CDS Offset	12
6	Gain.....	12
7	Full well capacity	14
8	Linearity.....	16
9	Dark current.....	18
10	Readnoise	19
11	Uniformity of readout between readout channels	21
11.1	Readout noise per channel.....	21
11.2	Signal per channel	22
12	Persistence.....	23
13	Crosstalk	27
13.1	Interpixel crosstalk	27
13.2	Channel crosstalk.....	28
14	Bad pixel map.....	30
15	Appendix A	31

1 INTRODUCTION AND SCOPE

1.1 General

The PANIC-4K Focal Plane Array (FPA) consists of a monolithic 4K x 4K HAWAII-4RG array from Teledyne covering the instrument field of view with a sampling of 4096x4096 pixels.

This document summarizes the detector characterization and performance data as measured during the cryogenic cycles of 2022, including the last results from tests in 2024.

1.2 Discussed items

The general characteristics discussed are gain, full well capacity, linearity, read noise, dark current, persistence, and crosstalk. The reset behavior of the detector is also addressed, while the inherent non-linear behavior of the detector is described separately in RD2, along with a recipe for correction.

2 SETUP AND DATA

2.1 Instrument setup

For the final characterization, PANIC was in operational configuration (all optical elements and detector integrated). For the crosstalk and persistence measurements, the only difference was that the focal plane mask was mounted at the mirror structure entrance instead of the field stop.

To illuminate the detector, a halogen desk lamp was placed on top of the telescope adapter. To create different intensities, the desk lamp was placed either closer or farther apart from the entrance window.

2.2 Detector setup

The most important settings of the detector setup used are listed in Table 2-1.

Table 2-1: Detector settings

Parameter	H4RG
Vext / V (bit)	2.080078 (2130)
Dsub / V (bit)	0.600179 (1034)
Vreset / V (bit)	0.30009 (517)
Vbias gate / V (bit)	same as Dsub (see RD1)
Pixel clock (kHz)	100

2.3 GEIRS Versions and minimum integration times

GEIRS is a living software subject to regular updates (RD7). The characterization started using version trunk-r799M-26 (Feb 27 2022, 15:45:06) and finished using version trunk-r807M-76 (Feb 3 2025, 16:28:17). The minimum integration times for those versions are listed below. All versions prior to trunk-r806M-154 (Nov 8 2024, 13:36:24) have a minimum integration time of ~ 2.76 s, and starting with version trunk-r806M-154, a minimum integration time of ~ 2.9 s.

Table 2-2. Minimum integration times with respect to the GEIRS version

GEIRS version	Min itime (s)	Readout mode	Comments
trunk-r799M-26	2.758022	cntsr	1x reset
trunk-r807M-76	2.903616	cntsr	10x resets (default)

2.4 Data

The characterization has been performed with different datasets, all using the **cntsr readout mode (only one recommended for operation)**. In general, multiple exposures have been taken for each setting, and averaged with median, unless noted otherwise.

3 SUMMARY

Table 3-1 summarizes the results obtained with the recommended readout mode (cntsr).

Table 3-1: Summary of characterization results with the cntsr readout mode

Parameter	Measured (MPIA)	GEIRS Version
Gain (e-/ADU)	2.3	trunk-r799M-26 (Feb 27 2022, 15:45:06) trunk-r806M-154 (Nov 8 2024, 13:36:24)
Full well (e-)	107201 (46609 ADU)	trunk-r799M-26 (Feb 27 2022, 15:45:06) trunk-r805M-57 (May 3 2024, 20:08:21) trunk-r806M-154 (Nov 8 2024, 13:36:24)
Linearity error < 5% (ADU)	1866 to 35000	trunk-r799M-26 (Feb 27 2022, 15:45:06) trunk-r805M-57 (May 3 2024, 20:08:21) trunk-r806M-154 (Nov 8 2024, 13:36:24)
Linearity error < 1% (ADU)	3733 to 27996	
Dark current mean (e-/s)	0.049	trunk-r807M-76 (Feb 3 2025, 16:28:17)
Readnoise / e-	15.9 ± 2.9	trunk-r799M-49 (Mar 22 2022, 14:27:12) trunk-r806M-154 (Nov 8 2024, 13:36:24)
Persistence (%) (5 min after saturation)	0.0102	trunk-r800M-11 (May 31 2022, 12:38:26)
Pixel crosstalk (%) (upper+lower)	1.81	trunk-r800M-11 (May 31 2022, 12:38:26)
Channel crosstalk (%) (saturated spot, worst case)	3.90	trunk-r800M-11 (May 31 2022, 12:38:26)

4 RESET LEVEL DRIFT

The reset level corresponds to the offset level of the detector signal after a reset is applied to all its pixels. In double correlated read, the reset level frame corresponds to the first frame that is read before the signal integration occurs, and it is the offset signal value that is subtracted on a pixel-by-pixel basis to obtain the resulting image (double correlated image). The mean signal of the reset frame should be the same for every image in a sequence with different integration times, because the photon collecting time in a reset frame is always identical to the time that is needed to apply the reset to all the detector pixels, which is independent of the commanded integration time.

However, the reset level drifts with increasing illumination, and the behaviour is different from readout mode to readout mode (RD4), as observed in Figure 1.

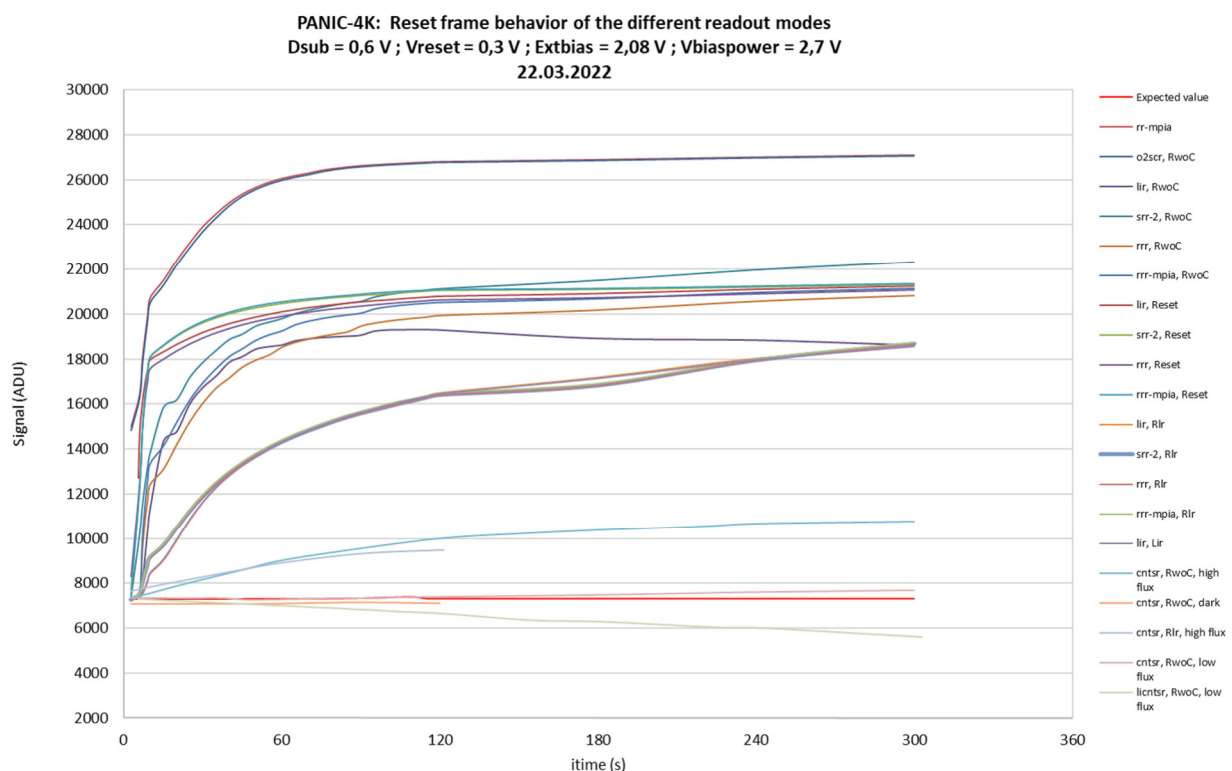


Figure 1. Reset frame behavior with different readout modes

The expected reset frame level should remain constant at about 7000 counts along the time axis (red line). However, the reset level varies drastically, up to ~ 20000 counts within 10 s.

Despite an extensive test phase with different approaches to reduce the drift (different readout modes with different clocking schemes while in idle, different reset times, different number of resets before the exposure), the best case obtained was with the cntsr readout mode and RwoC idle mode (RD4). This is why the only recommended readout mode for PANIC-4K is the cntsr. The behavior of the reset frame with the cntsr readout mode is shown in Figure 2.

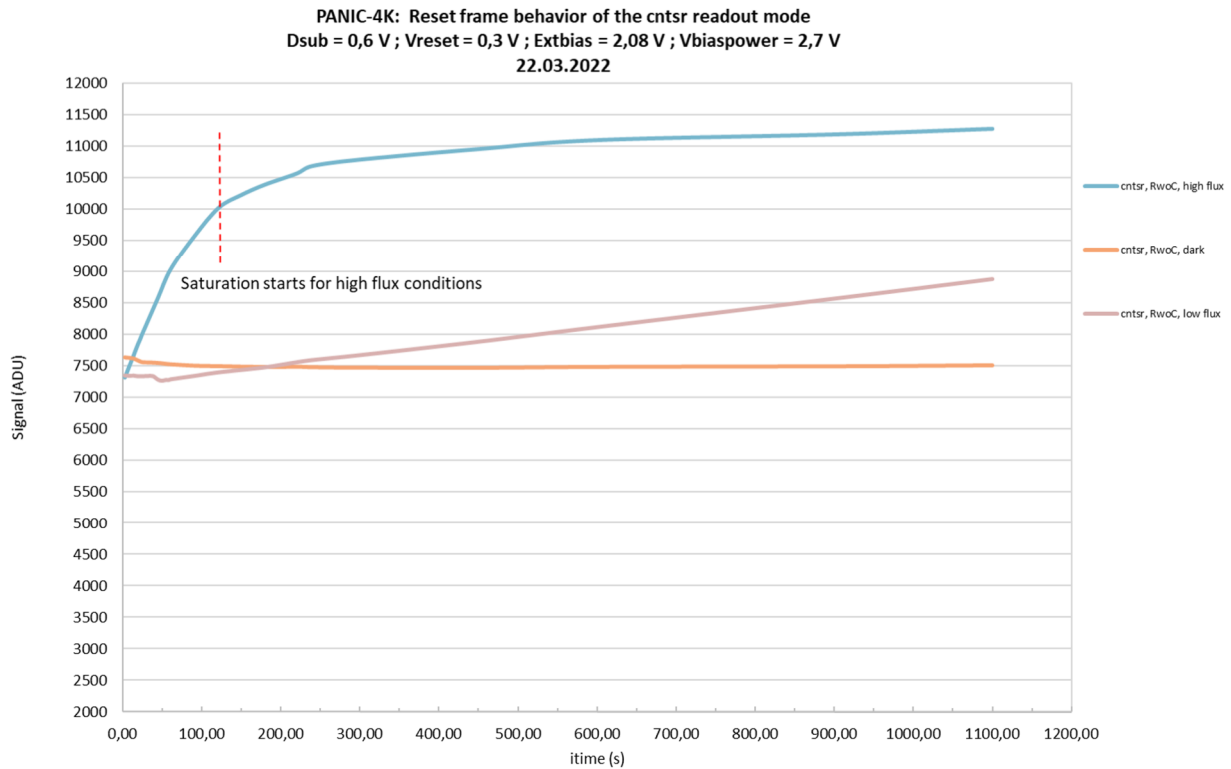


Figure 2. Reset frame behavior with the cntsr readout mode

The figure above shows the behavior of the reset frame with the cntsr mode (1x reset) for 3 different illuminating conditions: high flux (1750 ADU mean signal at minimum DIT in cntsr 2), low flux (80 ADU mean signal at minimum DIT in cntsr 2), and dark conditions. For both high and low flux conditions, the offset level starts at about 7300 counts, and then drifts away with higher counts (in this case by increasing the integration time), even after saturation (high flux), although the increase rate is much lower once passed this point. The offset level for dark conditions is slightly higher, possibly due to persistence effects of previous measurements. It is not yet understood, why the counts level for the low flux conditions remain constant until about 40 s and then slightly drop to start increasing with time at a constant rate.

Further analysis shows that the reset increase is also pixel wise; this means that for an image with an illuminated bright spot, the corresponding reset frame shows higher counts for the pixels where the spot is positioned. An example is shown in Figure 3 with a saturated and non saturated star of NGC891 taken during commissioning in February 2024. The upper green curve corresponds to the last frame of the exposure, while the lower blue curve to the reset frame. The reset level of the pixels where the star is positioned is higher than the neighbour pixels.



**Figure 3. Reset frame behavior (1x reset) of pixels corresponding to the position of bright stars.
Top: non-saturated star. Bottom: saturated star**

The analysis was repeated for different number of resets before the exposure. For these tests, the illumination was kept constant (halogen lamp at 1.08 V so that the detector saturates at 120 s) varying only the integration time. The results show that the behavior of the reset frame improves with increasing number of resets.

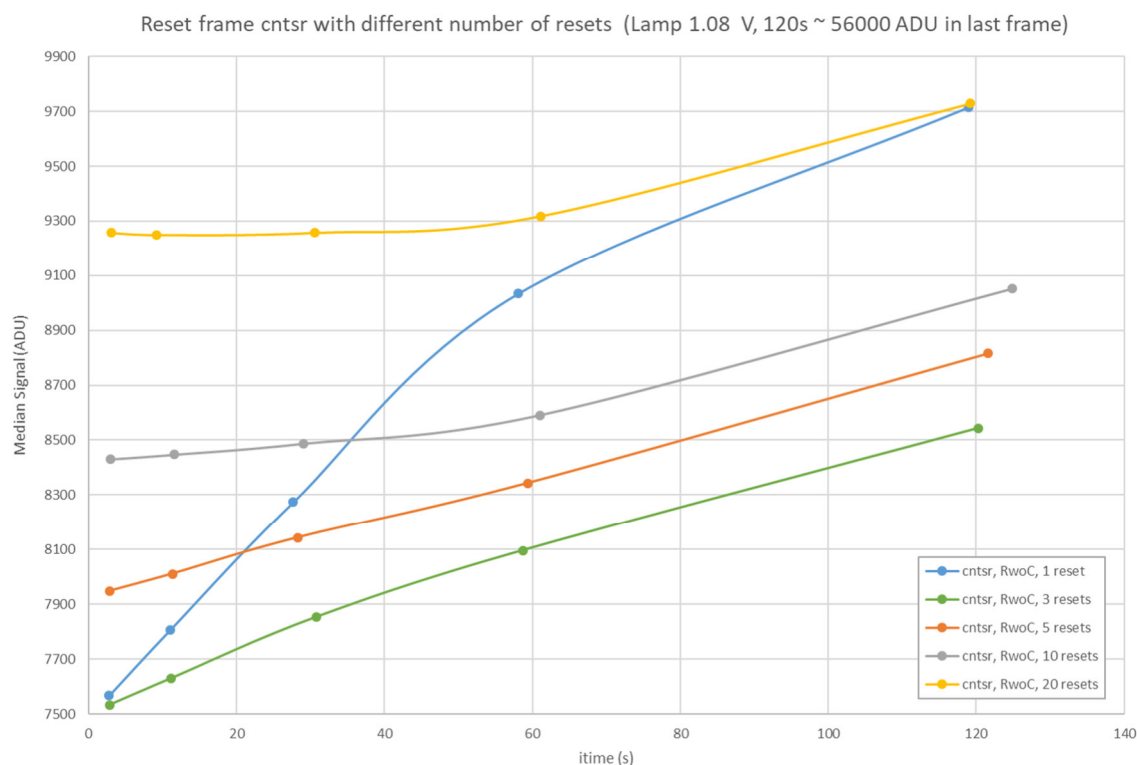


Figure 4. Reset frame behavior with different number of resets before the exposure

Figure 4 shows the behavior of the reset frame of the cntsr readout mode with different number of resets before the exposure. The blue curve shows the behavior with 1x reset, the green one with 3x resets, the orange one with 5x resets, gray for 10x resets and yellow for 20x resets. Even though the reset frame is not constant, an improvement is clearly observed when increasing the number of resets. The following table shows the total amount of reset drift from minimum integration time until saturation for the different cases:

Table 4-1: Total amount of drift in reset frame for different resets before the exposure

Case	Min itime (s)	Total amount of drift (ADU)
1x reset	2.765469	2146
3x resets	2.796169	1010
5x resets	2.826868	868
10x resets	2.903616	620
20x resets	3.057113	472

Table 4-1 shows the total amount of drift of the reset frame from minimum integration time until saturation for the different reset cases. It seems that further increase in the number of resets would lower the drift even more, but at the cost of larger minimum integration times. For this reason, it was decided that a good compromise between the minimum integration time and the achieved reset frame performance was with 10x resets. This is the PANIC new default.

For the purpose of completeness, saturated and non-saturated stars of NGC752 taken during commissioning in December 2024 were analysed using the new 10x resets default. The upper green curve corresponds to the last frame of the exposure, while the lower blue curve to the reset frame. In this case, with 10x resets before the exposure, the reset level of the pixels where the star is located does not increase, proving the efficiency of the 10x resets default.



Figure 5. Reset frame behavior (10x resets) of pixels corresponding to the position of bright stars. Top: non-saturated star. Bottom: saturated star

5 CDS OFFSET

The detector shows another anomaly in the form of electronic CDS offset due to the observed bias drift in the reset frame (chapter 4). This means that the reset frame has more counts than the consequent frames, as observed in the following figure:

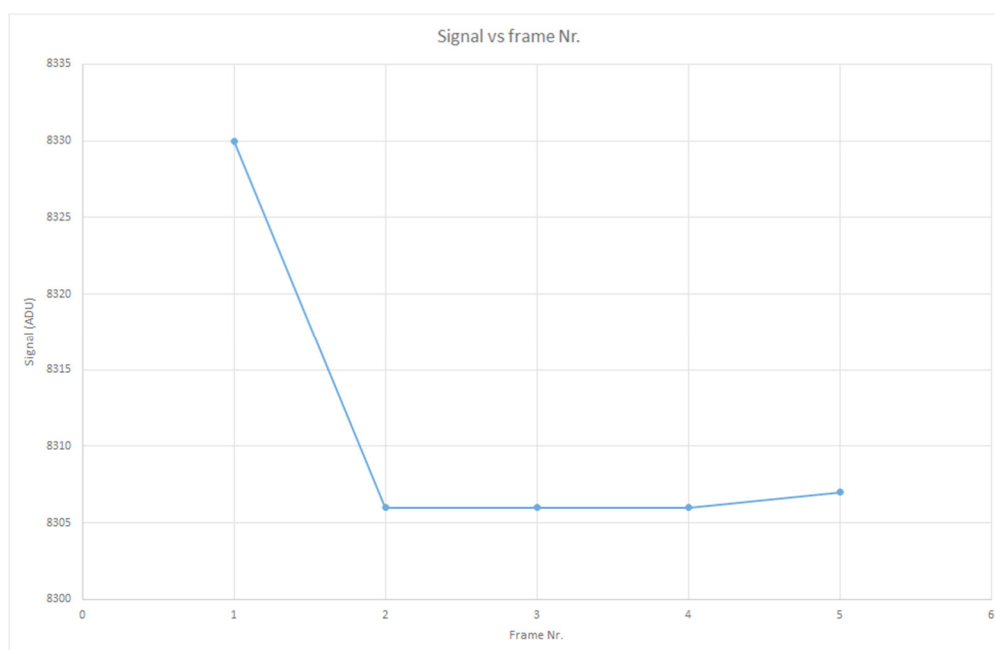


Figure 6. Median signal of a dark exposure with the cntsr 5 readout mode (5 frames in total, integration time = 11.6 s). The first frame (right after the 10x resets) shows higher counts, while the following frames are stable, dark signal slowly increasing (as expected).

Consequently, since the last frame has less counts than the first frame under dark conditions, the resulting CDS image (last frame minus reset frame) has a negative median value of approximately -30 ADUs. Meaning that all dark ramps start with a non-zero CDS offset of about -30 ADUs (RD6).

6 GAIN

The system gain relates the analog digital units (ADU) to the corresponding input electrons collected at the pixel unit cell, and it is expressed in units of electrons / ADU (e-/ADU). The system gain was calculated using the Photon Transfer Curve (variance vs. signal), keeping the illumination constant (halogen lamp, H and Ks filters) and varying only the detector integration time. The calculation was done for the whole array in a pixel-by-pixel basis under high and low flux conditions (1680 ADU and 75 ADU mean signal at minimum DIT in cntsr 2 respectively), obtaining two slightly different gain values for each case. The corresponding curves are presented below. The numbers are listed in Table 6-1.

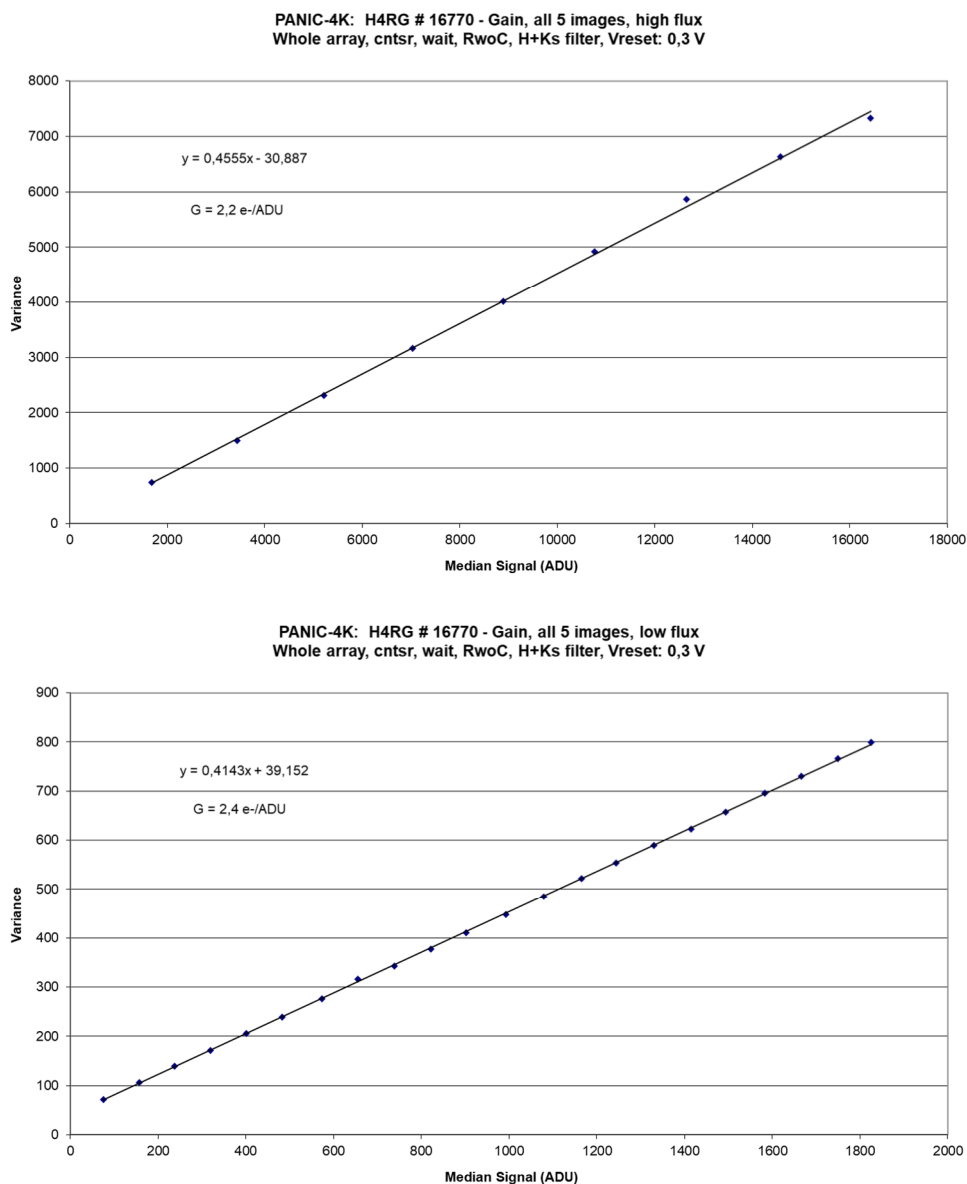


Figure 7: PTC for gain measurement, cntsr mode (1 reset), high flux (top) and low flux (bottom)

The measurement was repeated with 10x resets at the beginning of the exposure and using only the H-filter. The results show that the number of resets does not affect the system gain.

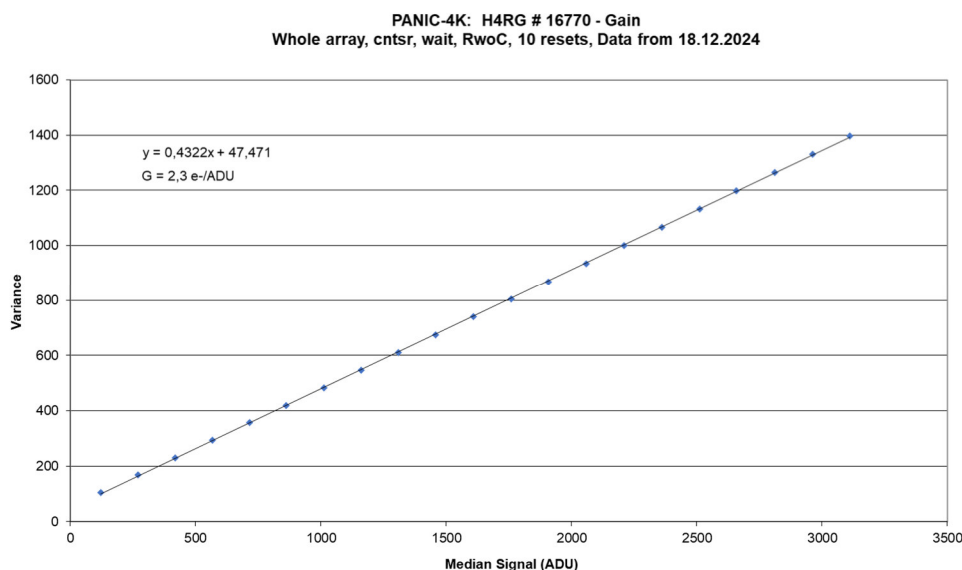


Figure 8. PTC for gain measurement, cntsr mode with 10x resets

Table 6-1: Measured gain values

Readout Mode	Gain (e-/ADU) (low flux, 1x reset)	Gain (e-/ADU) (high flux, 1x reset)	Gain (e-/ADU) 10x resets	Gain (e-/ADU) AVG
cntsr	2.1954	2.4137	2.3137	2.3076

7 FULL WELL CAPACITY

The full well capacity was calculated by keeping the illumination constant (halogen lamp) and varying only the detector integration time. For each exposure time, the median value of the signal detected was calculated. The procedure was done at MPIA with the H and Ks filters (both at the same time), and then repeated at CAHA (Coudé Room) for the H and Y filters (individually) with 1x reset, and again for the H filter with 10x resets. The full well corresponds to the saturation level reached at the highest integration times (Figure 9 and 10). The results show that the number of resets does not influence the full well capacity. The numbers are listed in Table 7-1.

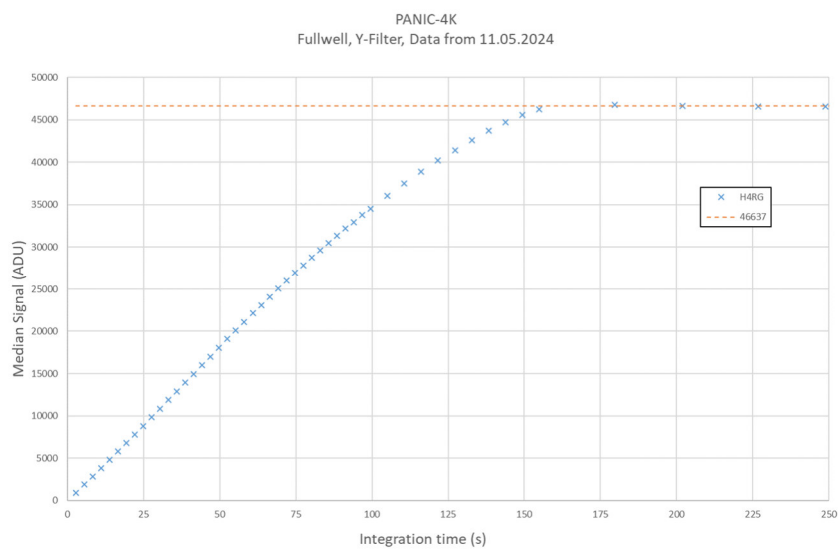
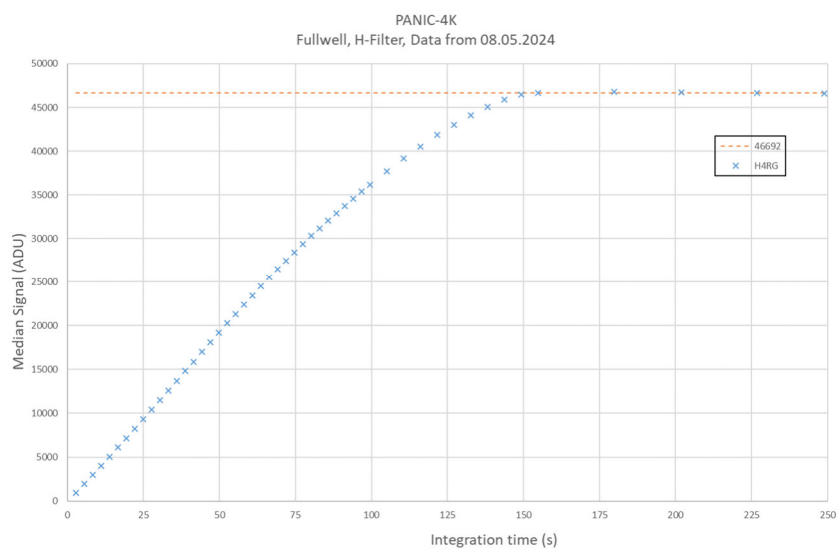
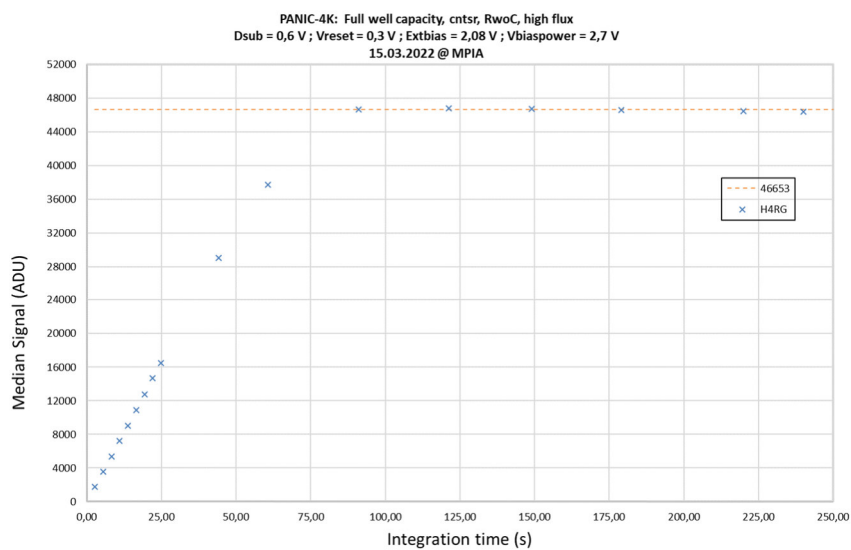


Figure 9: Median flatfield data for increasing itimes, cntsr mode, 1x reset. H+Ks (top), H (center), Y (bottom)

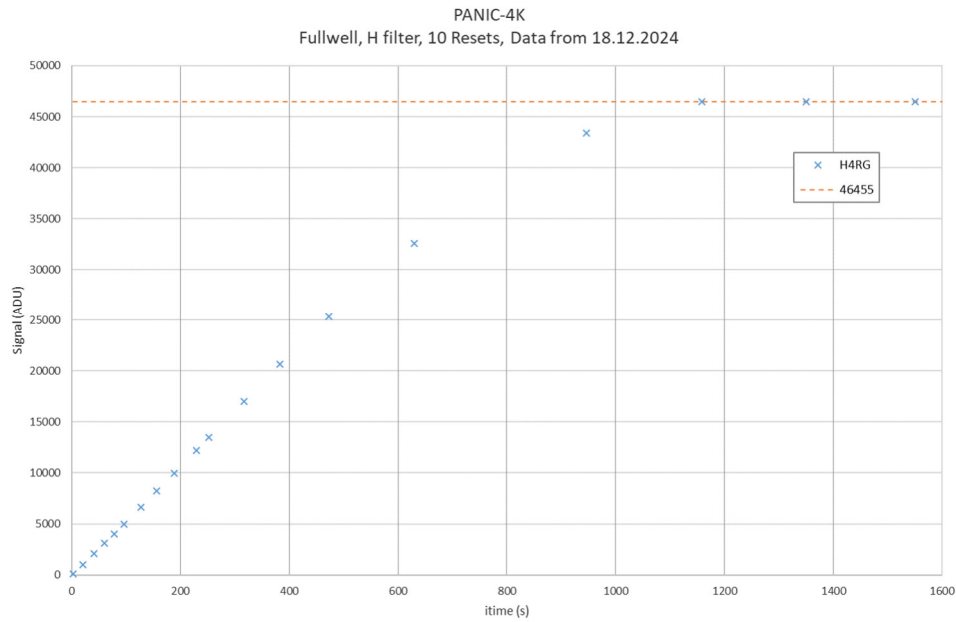


Figure 10. Median flatfield data for increasing integration times in cntsr mode with 10x resets

Table 7-1: Median CDS full well capacity in the cntsr readout mode

Full well		H + Ks (1x reset)	H (1x reset)	Y (1x reset)	H (10x resets)
cntsr median	ADU	46653	46692	46637	46455
	e ⁻	107301	107392	107264	106847

The average full well is reached at 107201 e⁻ (46609 ADU).

8 LINEARITY

The linearity behaviour of the detector (Figure 11) was calculated out of the full well capacity data presented in the previous section (cntsr, 1x reset). A linear fit ($y = mx+b$) from 10% to 60% of saturation shows that the detector is linear within 1% from 8% to 60% of the saturation value, and within 5% from 4% to 75% of saturation. The results are consistent with each other even though different filters were used. Comparable results were obtained for the case with 10x resets (Figure 12), as expected since the gain and full well capacity remained the same.

Details on the fit data can be found in Appendix A.

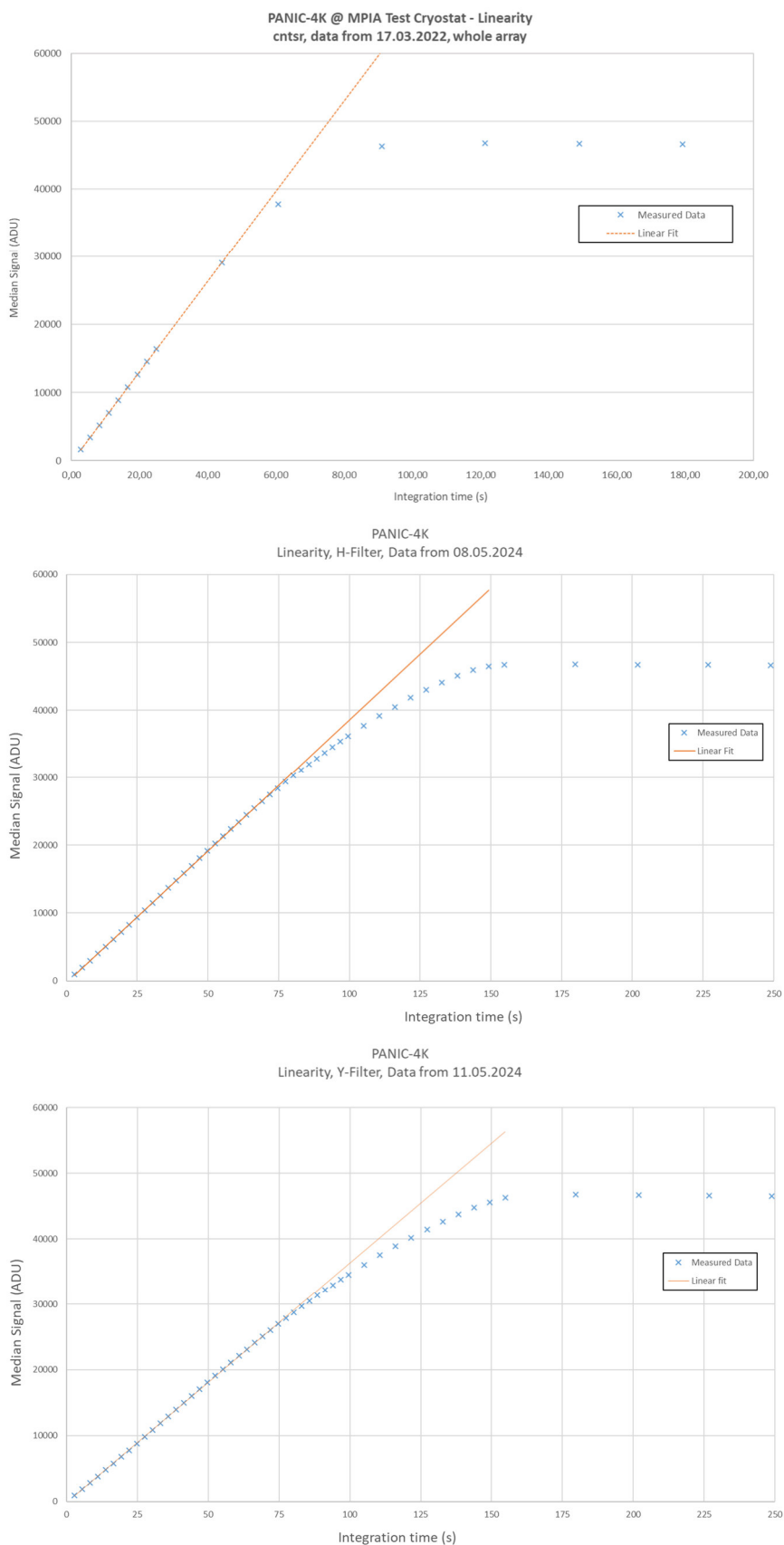


Figure 11: Linearity behavior with different filters (1x reset): H+Ks (top), H (center), Y (bottom)

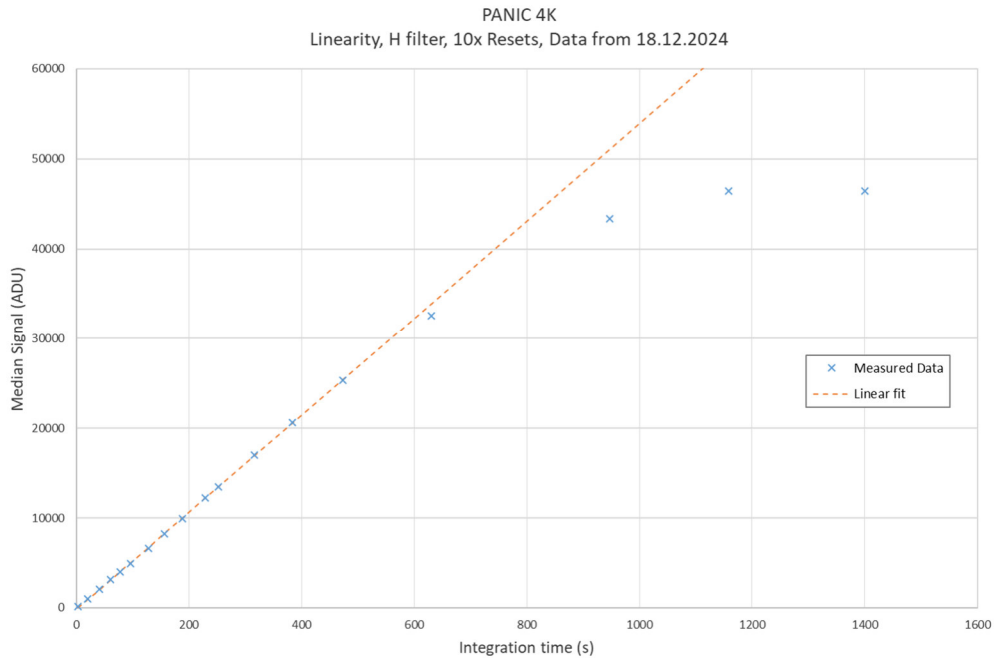


Figure 12. Linearity behavior with H filter (10x resets)

9 DARK CURRENT

Dark current is the signal generated by the detector under complete dark conditions. In order to achieve a light tight environment, all filter wheels were set to the “Blank” position. The dark current was calculated using a series of dark images taken with the cntsr readout mode (10x resets) at different detector integration times, going from minimum detector integration time until about 20 minutes. A slopes frame (ADU/s) was generated by adjusting a linear fit on a pixel-by-pixel basis for all the dark images (time axis). The calculated slopes were converted to electrons/s multiplying them by the system gain. The result is a histogram of the dark current as shown in Figure 13.

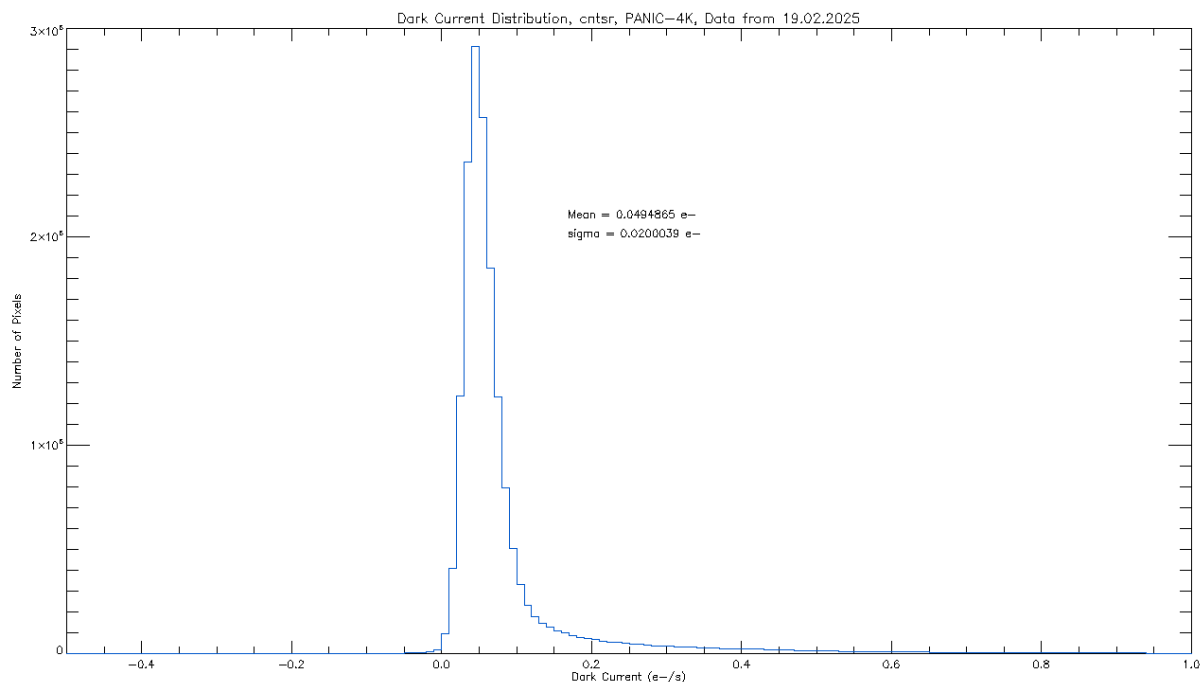


Figure 13: Dark current histogram, cntsr readout mode

Table 9-1: Measured dark current

Readout mode	Dark current mean (e-/s)
cntsr (10x resets)	0.049

It is important to mention that the measured dark current is 2.3 times larger than the value reported by Teledyne (RD3).

10 READNOISE

The readout noise (CDS) was calculated over a series of dark images obtained with minimum detector integration time and without any time interval between the individual images. A noise frame in ADU was generated by measuring the standard deviation for every pixel from all the dark images on a pixel-by-pixel basis. Then, the resultant noise frame was converted into electrons multiplying it by the system gain. The result is a histogram of the noise frame in electrons.

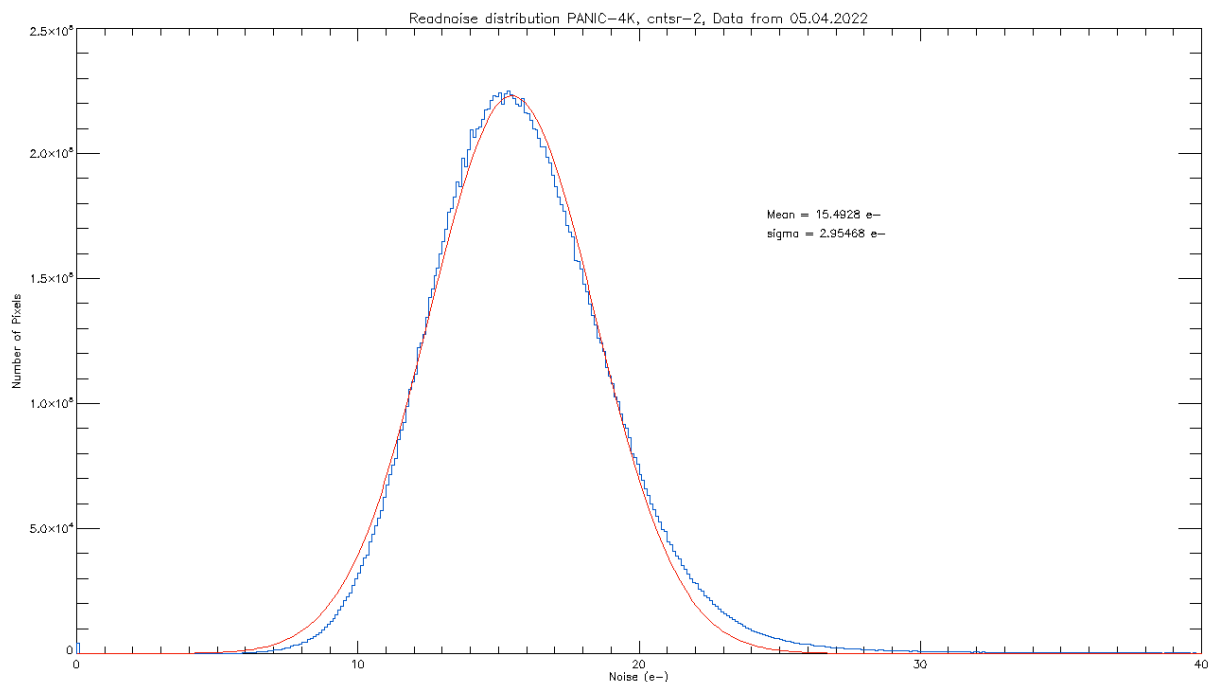


Figure 14: Read noise histogram (blue) and Gauss fit (red) with 1x reset

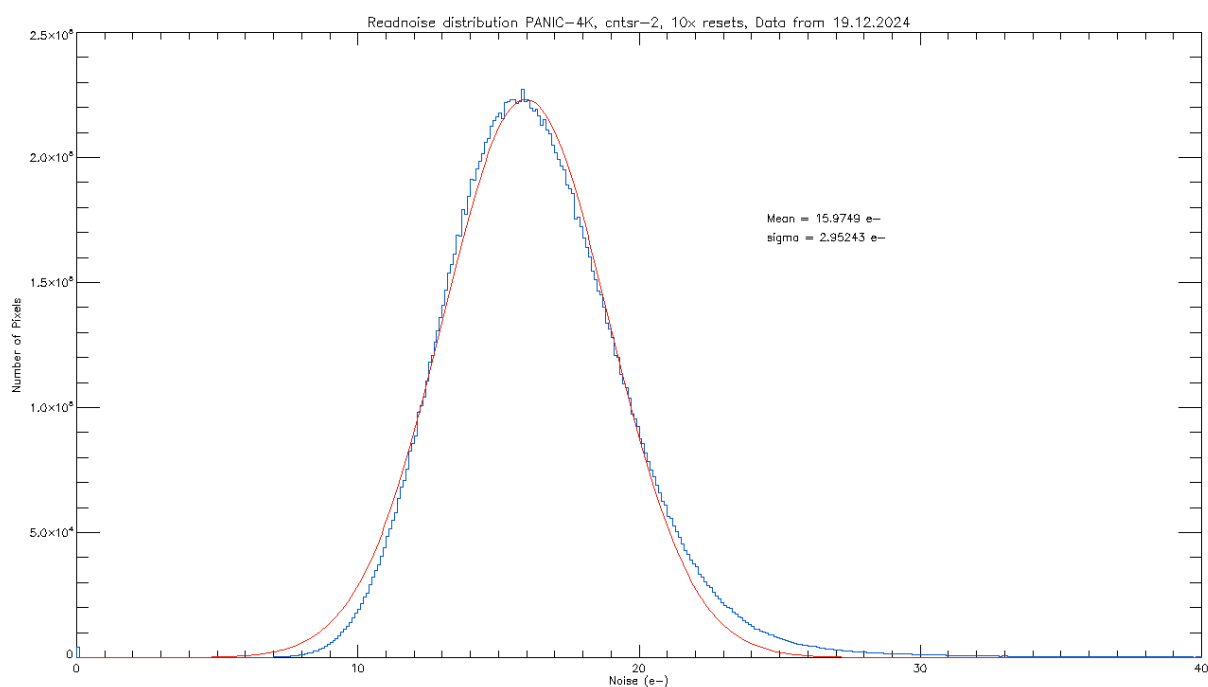


Figure 15. Read noise histogram (blue) and Gauss fit (red) with 10x resets

The figures above show the results obtained with 1x reset and 10x resets at the beginning of the exposure. By fitting the distribution with a Gaussian, it is observed that the distribution is slightly skewed towards larger values, but can be approximated with the Gaussian around the peak. The mean value is slightly larger for 10x resets, but still well below the requirements (RD5). Mean and width of the fitted curves are given in Table 10-1.

Table 10-1: CDS read noise, Gaussian fit mean and width

Readout mode	Readout noise (e-) 1x Reset	Readout noise (e-) 10x Resets
cntsr-2	15.49 ± 2.95	15.97 ± 2.95

11 UNIFORMITY OF READOUT BETWEEN READOUT CHANNELS

Since the detector is read out in 64 channel mode, it is interesting to know how do the channels behave individually. For this purpose, the readout noise per channel and the signal per channel were calculated.

11.1 Readout noise per channel

The readout noise per channel was obtained using the same noise frame as described in chapter 10, but calculating a histogram for every channel, where the mean of the histogram corresponds to the readout noise of the corresponding channel. The following figure shows the results obtained.

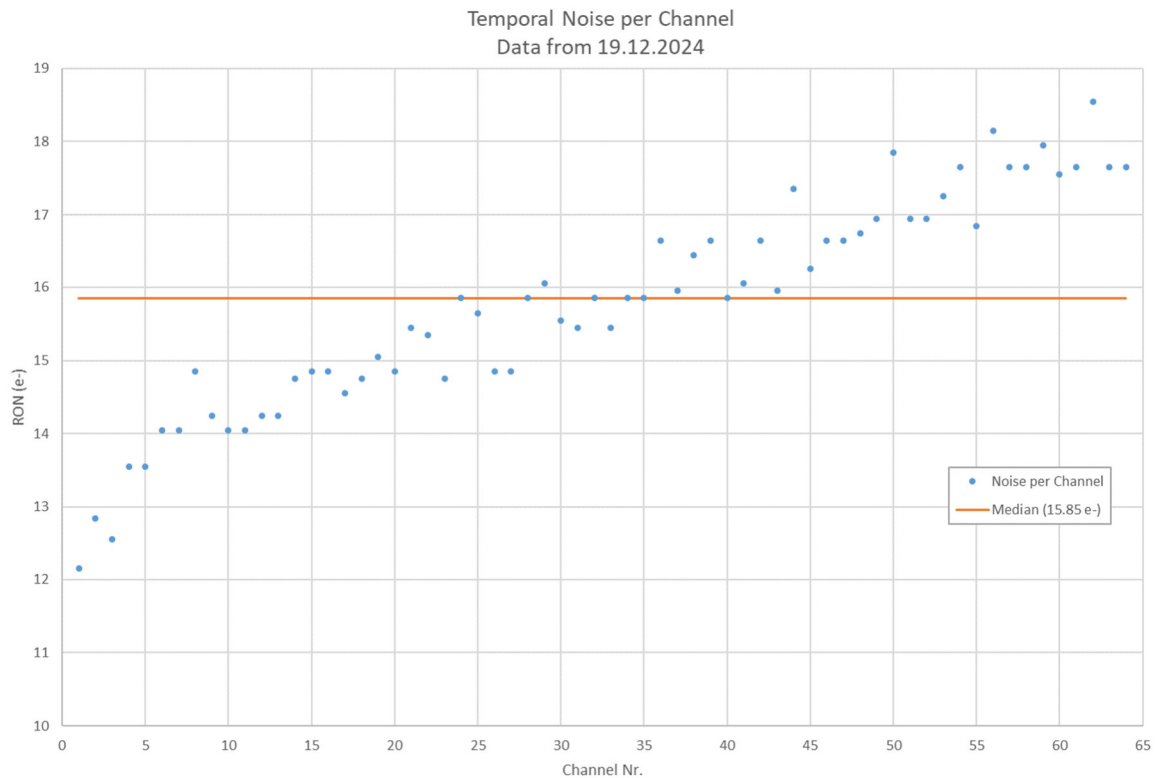


Figure 16. Temporal noise per channel

	PANIC4K detector characterization	Doc.Ref: PANIC4K-DET-TR-01 Issue: 1.0 Date: 30.05.2025 Page 22 / 33
---	--	--

The median of all channels (15.85 e-, orange line) is consistent with the value obtained in chapter 10. It can also be observed that the readout noise per channel varies between 12 e- and 19 e-, also consistent with the width of the Gaussian in Figure 15. The standard deviation of the noise values per channel corresponds to $\sigma = 1.45$ e-.

11.2 Signal per channel

The signal per channel was obtained from a 20000 ADU lab flat with the H filter and the halogen lamp at 0.5 V. The median signal per channel was calculated, results are shown in the following figure.

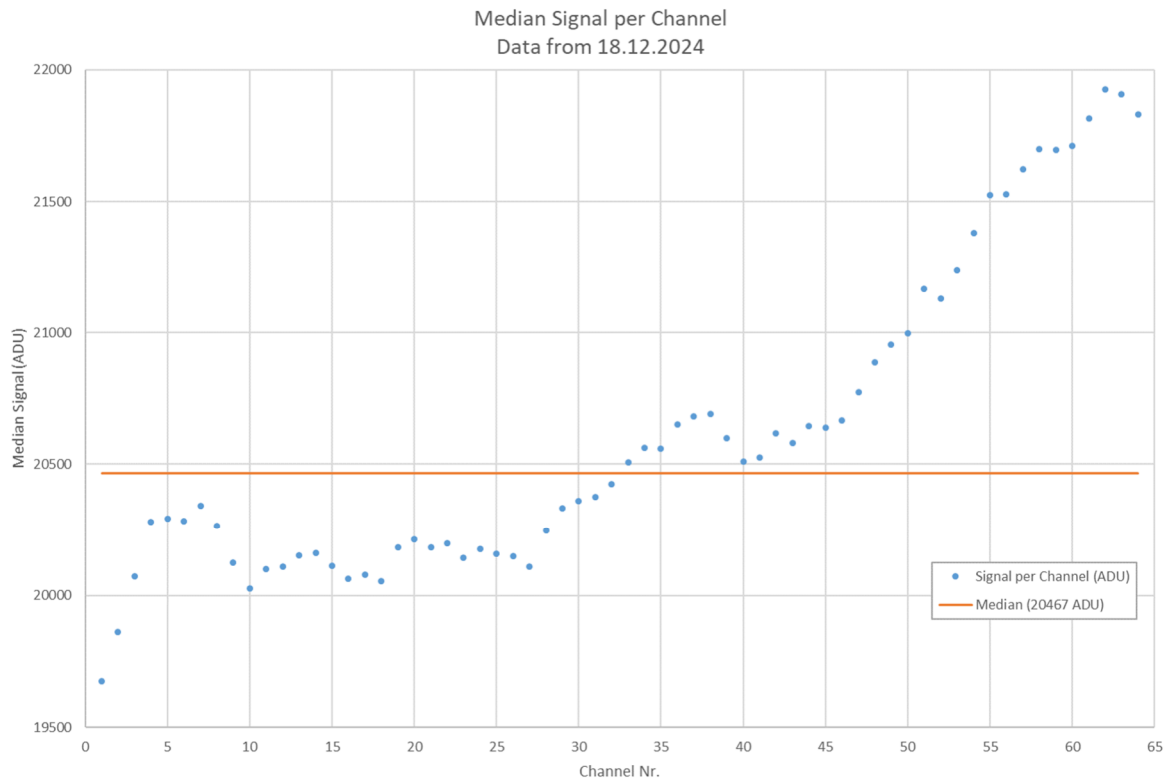


Figure 17. Median signal per channel

The signal per channel varies between 19600 ADU and 22000 ADU, while the median signal obtained corresponds to 20467 ADU, and the standard deviation of all channels is $\sigma = 581$ ADU. This means that the maximum deviation between the signal of the individual channels is less than 3σ , which corresponds to $\sim 7\%$ of the median signal.

12 PERSISTENCE

In order to measure persistence, exposures were taken with the cntsr readout mode (1x reset), the Ks filter and the focal mask at L1 installed. The pinhole images were analyzed, and compared to a non-illuminated background area. At first, 2 exposures were taken with 110,62 s (cntsr 41) to saturate the spots by about 10x. Then, with filters moved to BLANK, exposures of 11.06 s (cntsr 5) were taken for 35 min. The median signals of the areas analyzed are plotted in Figure 18, normalized to the average signal at the end of the measurement.

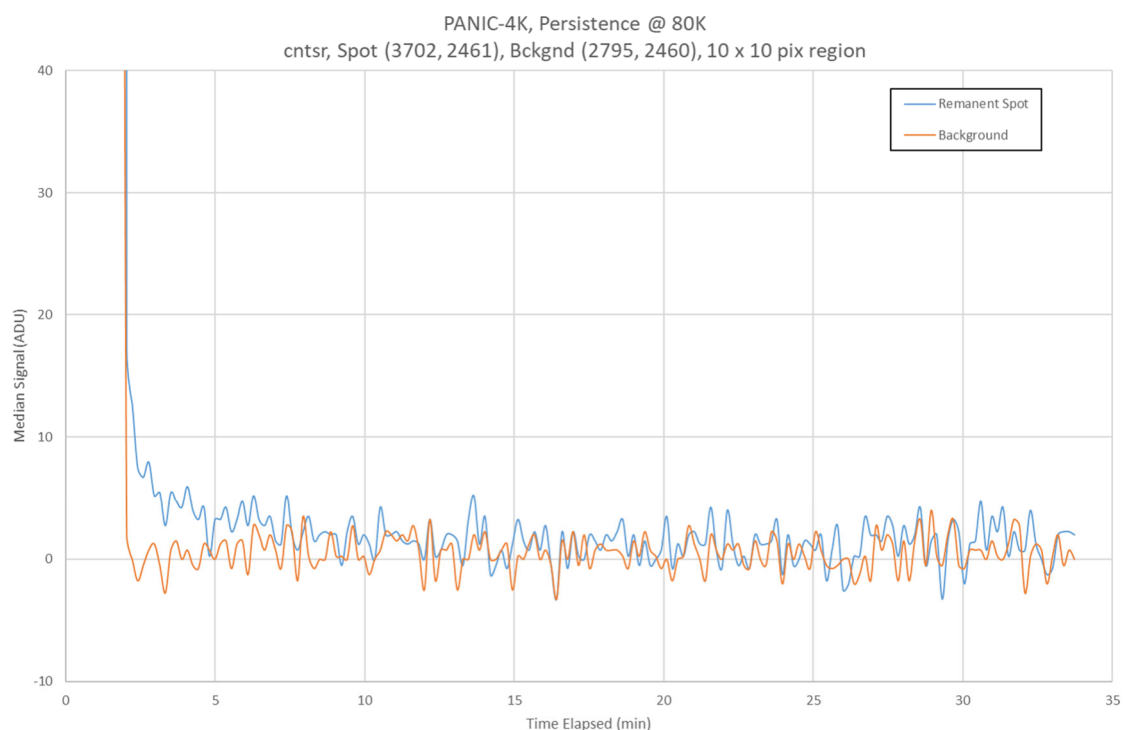


Figure 18: Persistence signal of 10x saturated spot during the first 30 min of 11s dark exposures

The counts return to the background level after 10 minutes. However, if the integration time is increased to 300 s, the spot remnant is still higher than the background by a factor of 1.7 (and decreasing with time) as observed in Figure 19.

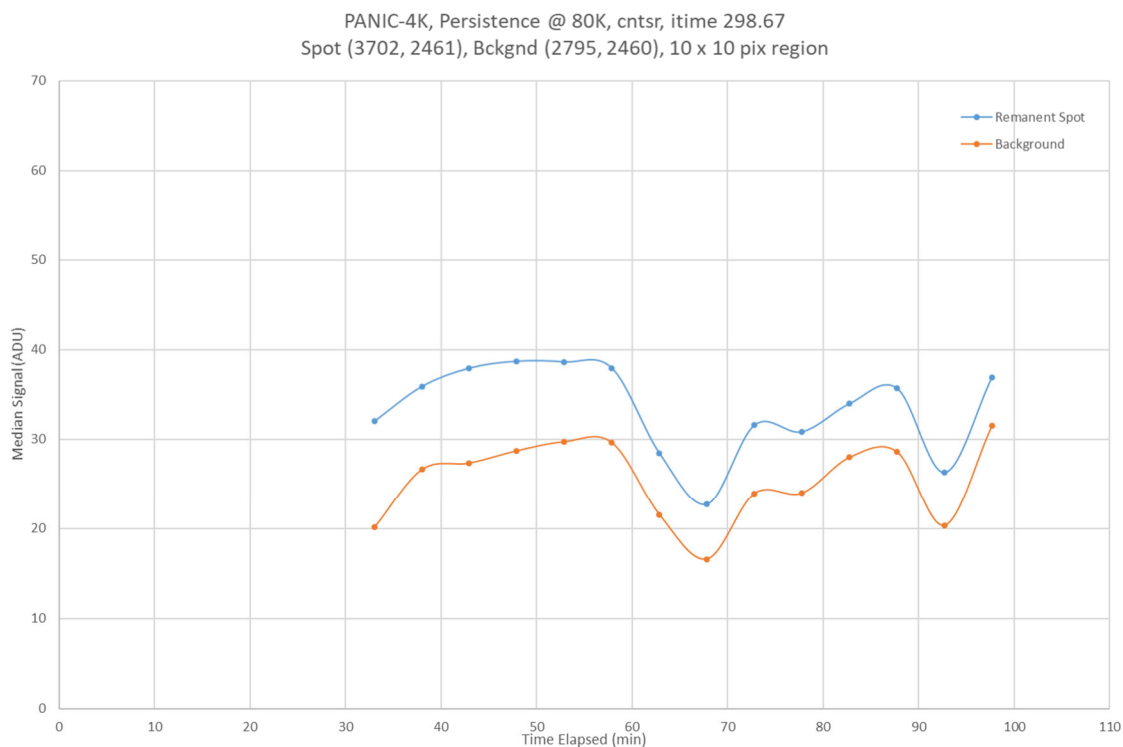


Figure 19: Persistence signal of 10x saturated spot after 30 min of 11s dark exposures. Data points taken with ~300 s dark exposures.

The signal fraction of the remnant spot investigated during the first 10 minutes of dark exposures is listed in Table 12-1.

Table 12-1: Persistence measurement, cntsr readout mode: intensity of remnant spot during the first 10 minutes of dark conditions

	Elapsed time after BLANKS set		Remnant spot %
Readmode	s	min	
cntsr	66.37128	1.106188	0.03559714
	121.68066	2.028011	0.02881673
	176.99008	3.134199	0.02203633
	188.05196	4.056022	0.03220694
	243.36136	5.162210	0.01017061
	365.04204	6.084034	0.01525592
	420.35144	7.005857	0.01356082
	486.72272	8.112045	0.01356082
	597.34152	9.955692	0.00847551
	608.4034	10.14005	0

A test on sky (NGC752) was also done using the H filter and cntsr with 10x resets. In this case, 7 exposures were taken with darks in between. The exposures were done with increasing integration time in order to fully saturate the stars. Then, with the filters moved to BLANK, dark exposures of 2.9 s (cntsr 2) were taken during a maximum of 2 min. The median signals of the star and background analyzed are plotted in Figure 20, normalized to the average signal at the end of the measurement. The signal fraction of the remanent spot during the dark exposures is listed in Table 12-2. The remanent spot is not visible to the eye after the dark exposures, but the results show that even after 20 s the remanent spot is still higher than the background by a factor of 1.7.

Therefore, it **is recommended** to take dark exposures with minimum integration time during at least 10 min after saturation occurs in order to get rid of persistence effects.

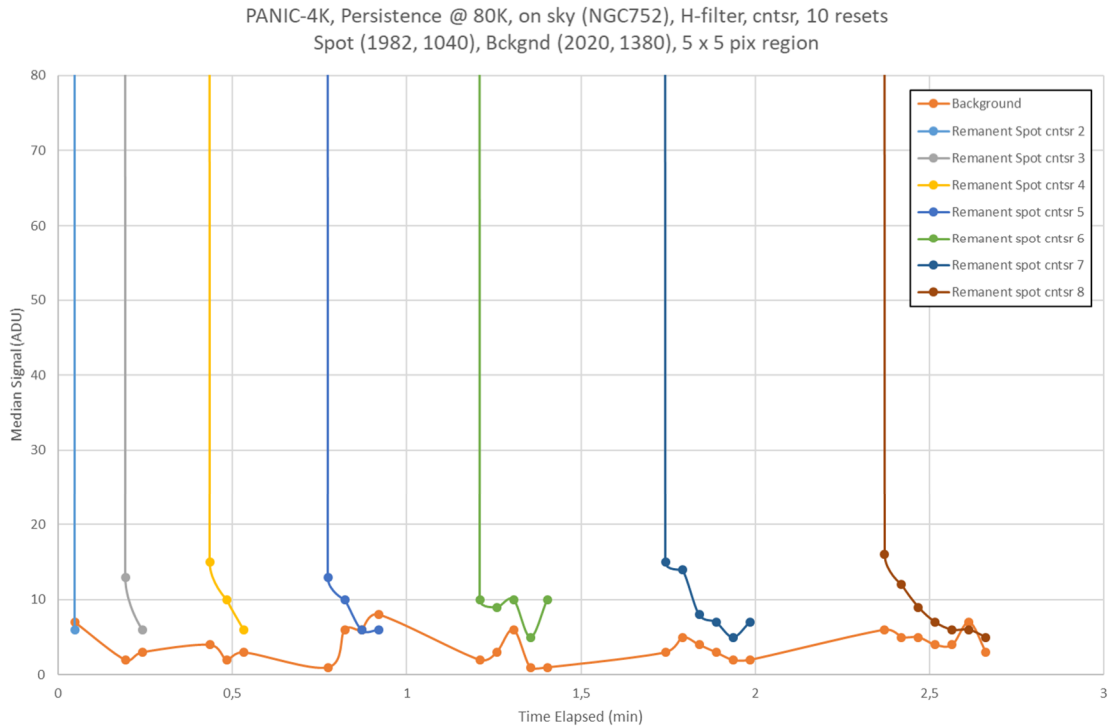


Figure 20. Persistence on sky (NGC752), H filter. Remanent signal with different integration times.

	PANIC4K detector characterization	Doc.Ref: PANIC4K-DET-TR-01 Issue: 1.0 Date: 30.05.2025 Page 26 / 33
---	--	--

Table 12-2. Persistence measurement on sky, cntsr readout mode: intensity of remnant spot during the first few seconds of dark conditions

Readout mode saturated star	Elapsed time after BLANKS set (s)	Remanent spot %	Factor remanent spot to background
cntsr 2	2.90362	0.012642758	0.86
cntsr 3	2.90362	0.027404191	6.5
	5.80724	0.012648088	2
cntsr 4	2.90362	0.031622887	3.75
	5.80724	0.021081924	5
	8.71086	0.012649155	2
cntsr 5	2.90362	0.027386871	13
	5.80724	0.021066824	1.67
	8.71086	0.012640094	1
	11.61446	0.012640094	0.75
cntsr 6	2.90362	0.021069043	5
	5.80724	0.018962139	3
	8.71086	0.021069043	1.67
	11.61446	0.010534522	5
	14.51808	0.021069043	10
cntsr 7	2.90362	0.031614889	5
	5.80724	0.029507229	2.8
	8.71086	0.016861274	2
	11.61446	0.014753615	2.33
	14.51808	0.010538296	2.5
	17.4217	0.014753615	3.5
cntsr 8	2.90362	0.033723259	2.67
	5.80724	0.025292444	2.4
	8.71086	0.018969333	1.8
	11.61446	0.014753926	1.75
	14.51808	0.012646222	1.5
	17.4217	0.012646222	0.86
	20.32531	0.010538518	1.67

13 CROSSTALK

13.1 Interpixel crosstalk

The pixel crosstalk is easily observed around hot pixels. One example image is shown in Figure 21. For the analysis, all the hot pixels of the array were selected and the percentage of the signal coupled to the direct neighbors calculated.

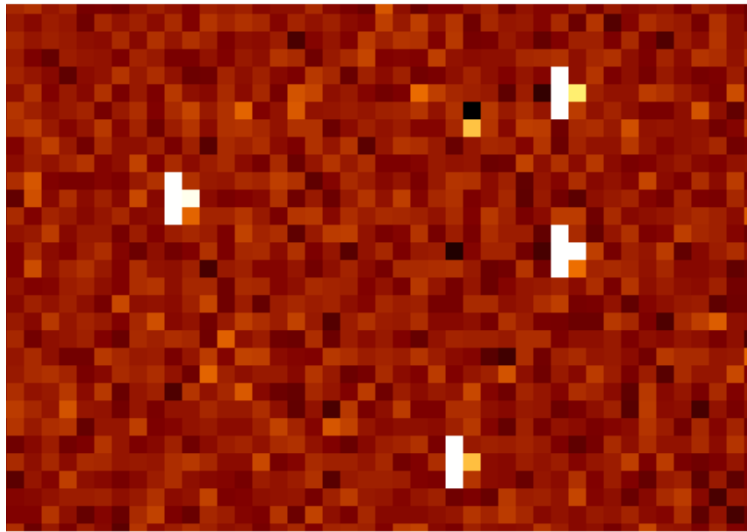
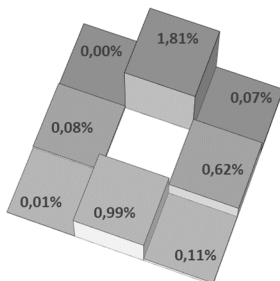


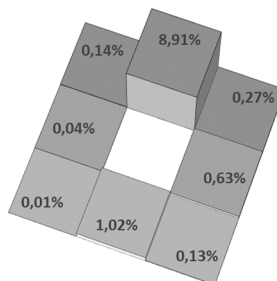
Figure 21: Example of pixel crosstalk around hot pixels, cuts: -50/100 ADU

The mean values of the neighboring pixels are shown in the following figures. Two other readout speeds were tested for completeness. As expected, faster readout rates increase the amount of pixel crosstalk.

Pixel Crosstalk at nominal 100 kHz pixel clock



Pixel Crosstalk at 200 kHz pixel clock



Pixel Crosstalk at 71 kHz pixel clock

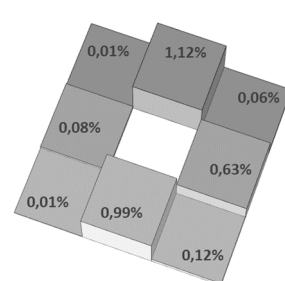


Figure 22: Pixel crosstalk at different readout speeds

There is a clear difference between the upper+lower and left+right direction. This is also observed in Figure 21, and most likely caused by the line reset used in PANIC. Note that the lower and left+right neighbor pixels barely change with the pixel clock. Only the upper neighbor pixel is affected by the readout speed.

13.2 Channel crosstalk

The channel crosstalk was measured with the focal mask installed at L1 and at different readout speeds. Spots in the image are taken at about saturation. For the analysis, the images were dark subtracted, and 8 bright spots were selected across the detector. Ghosts appearing in the other channels are compared to the bright spot (Figure 23). The results are listed in Table 13-1.

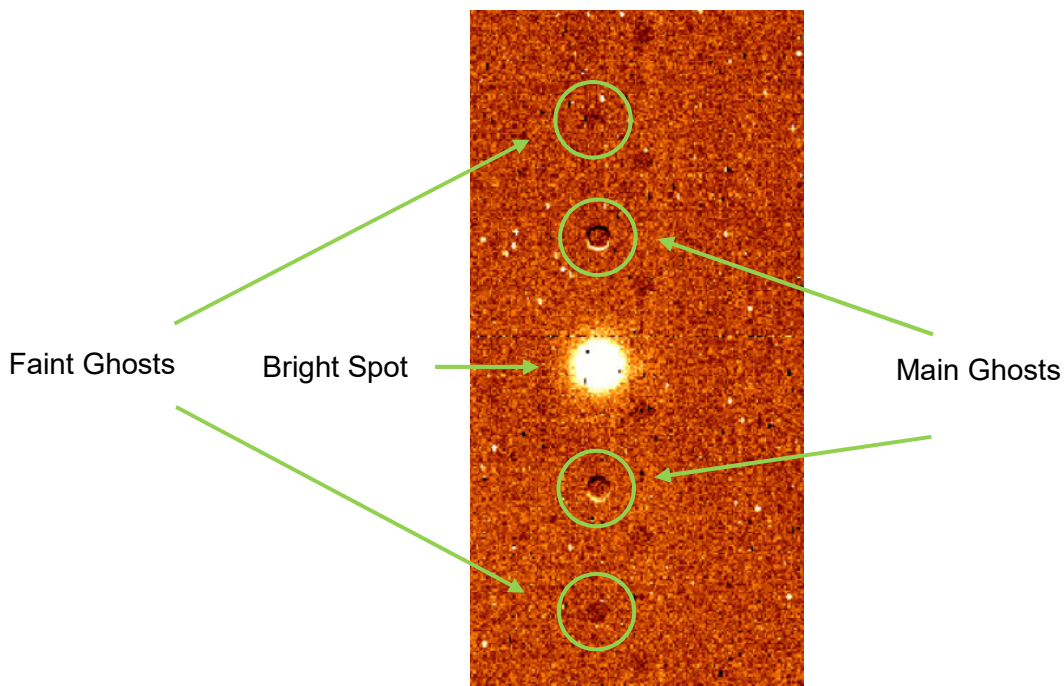


Figure 23: Image showing channel crosstalk at 200 kHz. The saturated bright spot (center) appears at the conjugated positions in the other channels with different intensities (faint and main ghosts)

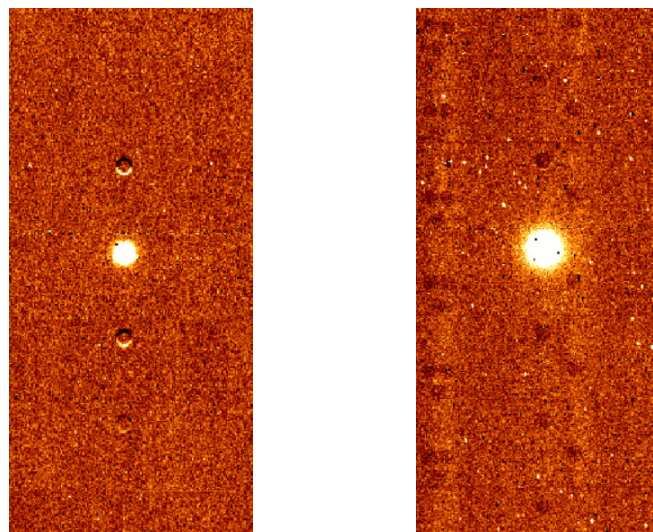


Figure 24: Channel crosstalk at 200 kHz pixel clock (left) and 71 kHz (right). The main ghosts fade to faint ghosts for lower readout speeds.

Table 13-1: Position of the spots used for the channel crosstalk analysis

Spot Nr.	Center Position (x, y)		
	Bright Spot	Main Ghost	Faint Ghost
1	(1707, 900)	(1707, 837)	(1707, 773)
2	(1307, 497)	(1307, 434)	(1307, 370)
3	(2182, 336)	(2182, 272)	(2182, 206)
4	(2782, 3601)	(2782, 3537)	(2782, 3473)
5	(3040, 3449)	(3040, 3385)	(3040, 3321)
6	(2866, 2859)	(2866, 2796)	(2866, 2731)
7	(2841, 1240)	(2841, 792)	(2841, 857)
8	(1049, 649)	(1049, 714)	(1049, 584)

Table 13-2: Main and faint ghosts, fraction of bright spot at different readout speeds

Spot Nr.	Fraction of bright spot (%)					
	200 kHz		100 kHz		71 kHz	
	Main	Faint	Main	Faint	Main	Faint
1	6.42	5.60	3.20	3.90	1.20	1.00
2	6.40	2.90	1.80	1.10	1.30	2.40
3	4.30	2.60	1.70	0.90	1.10	1.20
4	3.20	2.20	0.90	0.60	1.40	1.80
5	8.20	5.10	2.20	1.40	0.80	0
6	6.30	3.60	2.20	1.20	1.50	0
7	7.10	3.30	1.50	0	1.30	1.20
8	17.30	9.20	7.40	3.70	0	3.20

The table above shows the main and faint ghosts as a fraction of the bright spot for different readout speeds. As expected, the ghosts are more visible at higher readout speeds. For the nominal pixel clock of 100 kHz, the larger ghosts are < 4% of the bright spot. Even though the ghosts' effects would be reduced by using slower pixel clocks, the minimum integration time would increase, making this option unattractive.

	PANIC4K detector characterization	Doc.Ref: PANIC4K-DET-TR-01 Issue: 1.0 Date: 30.05.2025 Page 30 / 33
---	--	--

14BAD PIXEL MAP

The following figure shows a bad pixel map of the detector, where all bad pixels (hot, cold, dead) are marked in red. Hot pixels were masked as bad if its value is larger than 360 ADU (10 times the mean of a dark exposure with minimum integration time). Cold pixels were considered as bad if its value is less than 3883 ADU (10% of the mean of a 1 minute exposure lab flat, filters: H, Ks), and pixels with a value of 0 were identified as electrically dead pixels.

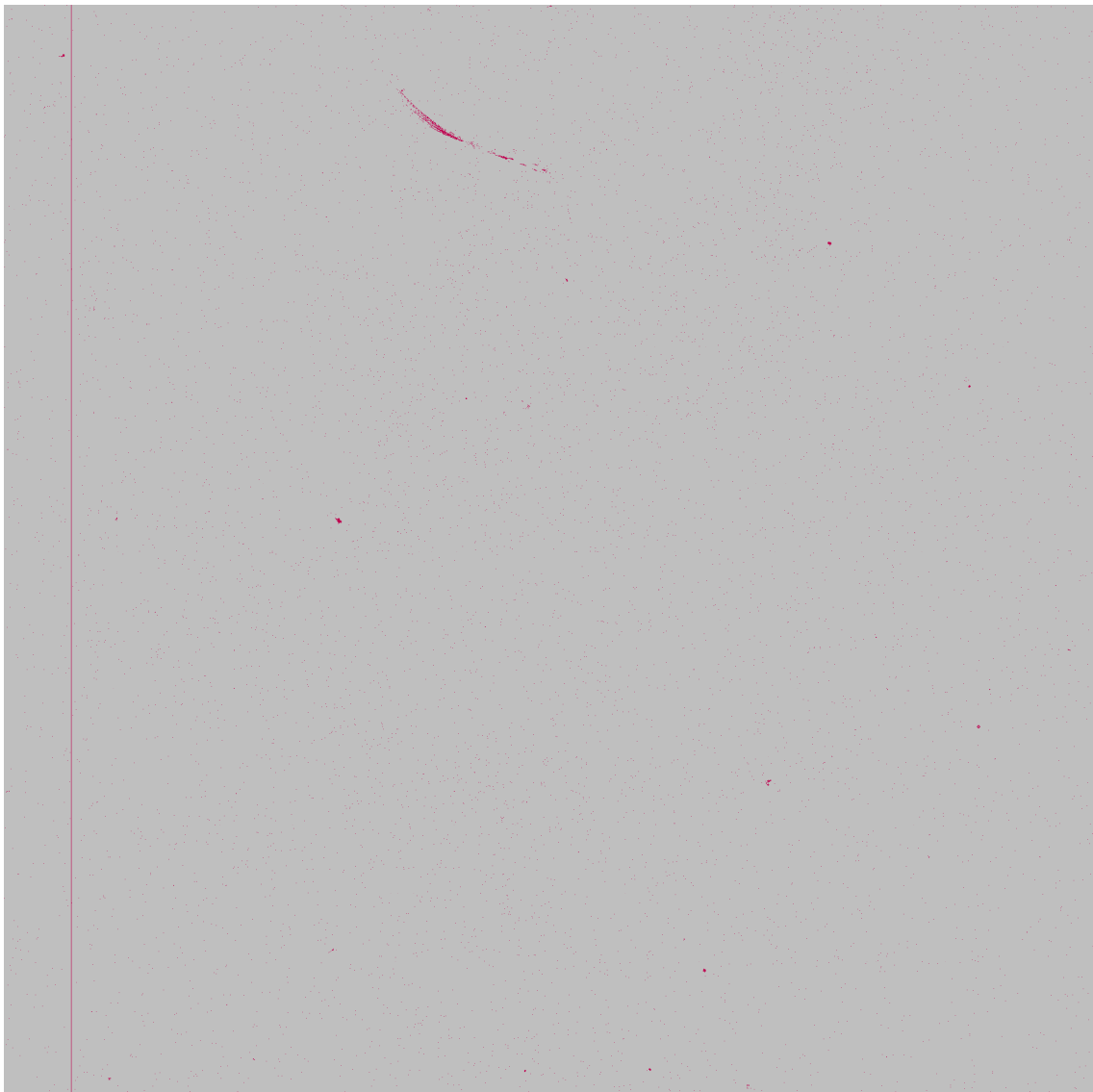


Figure 25: Bad pixel map, bad pixels marked in red

The information is stored in a FITS file, and also made available for GEIRS in a text file.

15 APPENDIX A

Data used for the linear fits of the linearity calculation.

Table 15-1: Parameters of the linear fits ($y = mx+b$) for the different filters

Filter	m	b	Comment
H+Ks	666.706	-251.668	1x reset
H	386.385	-249.674	1x reset
Y	365.397	-238.631	1x reset
H	54.123	-205.489	10x resets

Table 15-2: Linear fit and corresponding error with the H+Ks filters (1x reset)

itime (s)	Fit value (ADU)	% Error (abs)	% from sat value
2.76	1587.12	5.69	3.64
5.52	3425.91	0.18	7.42
8.27	5264.69	0.96	11.27
11.03	7103.48	0.91	15.22
13.79	8942.27	0.59	19.22
16.55	10781.06	0.13	23.29
19.31	12619.85	0.25	27.36
22.06	14458.64	0.79	31.52
24.82	16297.43	0.81	35.54
44.13	29168.95	0.34	62.87
60.68	40201.68	6.33	81.78
91.01	60428.36	30.42	100.22

Table 15-3: Linear fit and corresponding error with the H filter (10x reset)

itime (s)	Fit value (ADU)	% Error (abs)	% from sat value
2.903616	-48.33781195	351.5628968	-0.10405298
11.614464	423.1163246	33.95843107	0.910809008
20.325312	894.5704611	13.08220246	1.925670996
31.939776	1523.175976	5.687069311	3.278820313
40.650624	1994.630113	3.227159089	4.293682301
49.361472	2466.08425	1.845672971	5.308544289
60.975936	3094.689765	0.527039423	6.661693607
69.686784	3566.143901	0.004035212	7.676555595
78.397632	4037.598038	0.341737535	8.691417583
84.204864	4351.900796	0.507846955	9.367992241
95.819328	4980.506311	0.757081885	10.72114156
127.759104	6709.171478	0.881949113	14.44230218
156.795264	8280.685267	0.740094265	17.82517547
188.73504	10009.35043	0.471061877	21.5463361
229.385664	12209.46974	0.061179871	26.28235871
252.614592	13466.68077	0.150885223	28.98865734
316.494144	16924.0111	0.557331688	36.43097859
383.277312	20538.49282	0.555898646	44.21158716
473.289408	25410.18556	0.417885814	54.69849437
630.084672	33896.36002	3.877584548	72.96601016
786.879936	42382.53448	16.29554629	91.23352594



PANIC4K detector characterization

Doc.Ref:
Issue:
Date:
Page 32 / 33

PANIC4K-DET-TR-01
1.0
30.05.2025

Table 15-4: Linear fit and corresponding error with the H filter (1x reset)

Integration time (s)	Fit value (ADU)	% Error (abs)	% from sat value
2.765469	818.86	17.20	2.13
5.530938	1887.40	4.14	4.29
8.296408	2955.93	1.10	6.47
11.061878	4024.47	0.28	8.64
13.827347	5093.01	0.84	10.76
16.592816	6161.54	0.98	13.02
19.358285	7230.08	0.99	15.32
22.123754	8298.61	0.92	17.43
24.889223	9367.15	0.65	19.65
27.654692	10435.68	0.50	22.17
30.420161	11504.22	0.20	24.94
33.18563	12572.76	0.04	26.44
35.951099	13641.29	0.11	28.46
38.716568	14709.83	0.36	31.89
41.482037	15778.36	0.29	34.03
44.247506	16846.90	0.51	35.42
47.012975	17915.43	0.60	37.75
49.778444	18983.97	0.59	40.29
52.543913	20052.51	0.70	42.71
55.309382	21121.04	0.58	45.49
58.074851	22189.58	0.48	48.34
60.84032	23258.11	0.40	50.61
63.605789	24326.65	0.26	51.94
66.371258	25395.18	0.04	53.17
69.136727	26463.72	0.33	54.68
71.902196	27532.26	0.64	56.78
74.667665	28600.79	1.05	59.69
77.433134	29669.33	1.35	63.14
80.198603	30737.86	1.82	65.67
82.964072	31806.40	2.47	67.46
85.729541	32874.93	2.89	68.80
88.49501	33943.47	3.47	69.61
91.260479	35012.01	4.08	70.48
94.025948	36080.54	4.57	71.57
96.791417	37149.08	5.16	72.96
99.556886	38217.61	5.71	74.95
105.087837	40351.66	6.95	79.47
110.618776	42492.23	8.23	82.40
116.149715	44628.94	9.59	85.41
121.680653	46765.65	10.88	88.98
127.211592	48902.98	12.40	92.00
132.742531	51040.05	13.91	94.74
138.27347	53177.12	15.50	97.87
143.804408	55314.19	17.38	100.12
149.335347	57451.26	19.54	101.56



PANIC4K detector characterization

Doc.Ref:
Issue:
Date:
Page 33 / 33

PANIC4K-DET-TR-01
1.0
30.05.2025

Table 15-5: Linear fit and corresponding error with the Y filter (1x reset)

Integration time (s)	Fit value	% Error (abs)	% from sat value
2.765469	771.86	19.30	1.97
5.530938	1782.36	5.07	4.02
8.296408	2792.85	1.54	6.08
11.061878	3803.35	0.05	8.16
13.827347	4813.85	0.64	10.26
16.592816	5824.34	0.89	12.38
19.358285	6834.84	0.94	14.52
22.123754	7845.33	0.92	16.67
24.889223	8855.83	0.74	18.85
27.654692	9866.32	0.58	21.03
30.420161	10876.82	0.40	23.23
33.18563	11887.31	0.20	25.44
35.951099	12897.81	0.08	27.63
38.716568	13908.30	0.06	29.84
41.482037	14918.80	0.19	32.05
44.247506	15929.29	0.31	34.26
47.012975	16939.79	0.47	36.49
49.778444	17950.28	0.61	38.73
52.543913	18960.78	0.66	40.92
55.309382	19971.27	0.66	43.11
58.074851	20981.77	0.67	45.29
60.84032	21992.26	0.61	47.44
63.605789	23002.76	0.45	49.54
66.371258	24013.25	0.37	51.68
69.136727	25023.75	0.17	53.75
71.902196	26034.24	0.09	55.77
74.667665	27044.74	0.35	57.79
77.433134	28055.23	0.69	59.74
80.198603	29065.73	1.06	61.66
82.964072	30076.22	1.44	63.56
85.729541	31086.72	1.85	65.42
88.49501	32097.21	2.34	67.22
91.260479	33107.71	2.80	69.00
94.025948	34118.20	3.36	70.70
96.791417	35128.70	3.86	72.42
99.556886	36139.19	4.38	74.09
105.087837	38160.19	5.49	77.33
110.618776	40181.18	6.66	80.42
116.149715	42202.17	7.86	83.38
121.680653	44223.16	9.10	86.20
127.211592	46244.15	10.38	88.87
132.742531	48265.14	11.70	91.38
138.27347	50286.13	13.06	93.75
143.804408	52307.12	14.47	95.92
149.335347	54328.11	16.07	97.77
154.866286	56349.10	17.94	99.16
179.755511	65443.56	28.55	100.26